Annals of Phytomedicine 13(2): 474-483, 2024

DOI: http://dx.doi.org/10.54085/ap.2024.13.2.47

Annals of Phytomedicine: An International Journal
http://www.ukaazpublications.com/publications/index.php

Print ISSN : 2278-9839 Online ISSN : 2393-9885

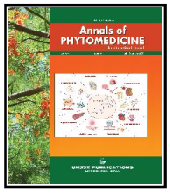

Original Article : Open Access

A computational study on anticarcinogenic activity of secondary metabolites in *Salvia rosmarinus* Spenn. against skin cancer

S. Tamilselvi◆, N.M. Saravanakumar*, G.V. Anjali, V. Gnana Asmi, K. Elango, J. Santhika and T. Prabha**

Department of Biotechnology, Bannari Amman Institute of Technology, Sathyamangalam-638401, Erode, Tamil Nadu, India

** Department of Information Technology, Karpagam College of Engineering, Othakkaal Mandapam-641032, Coimbatore, Tamil Nadu, India*

*** Department of Pharmaceutical Chemistry, Nandha College of Pharmacy, Affiliated with The Tamil Nadu Dr. MGR Medical University, Chennai, Erode-638052, Tamil Nadu, India*

Article Info

Article history
Received 2 October 2024
Revised 19 November 2024
Accepted 20 November 2024
Published Online 30 December 2024

Keywords
Salvia rosmarinus Spenn.
DNA barcoding
Analytical techniques
Antioxidant activity
Molecular docking
Molecular dynamic study

Abstract

Salvia rosmarinus Spenn., commonly called Rosemary, is widely known for its medicinal and biological properties and belongs to the Lamiaceae family. It is anticancer and antioxidant properties are attributed to the presence of carnosic acid, making it useful in the industrial sectors. The value-added economic plants are referred for their therapeutic and cosmetic importance. This study aims to validate the extraction method and explore the *in silico* potential of carnosic acid against skin cancer ligands. The *S. rosmarinus* sample was authenticated through DNA barcoding, and the effectiveness of various extraction methods, such as, Maceration, Soxhlet, and Ultrasonication was evaluated. The maximum carnosic acid content of 110 mg is extracted from the maceration technique. The high-efficiency extract was further characterized using FTIR, GC-MS, and HPLC, followed by an assessment of its antioxidant capacity. Molecular docking was performed to assess the therapeutic potential of carnosic acid in comparison with skin cancer ligands. High binding interactions were observed between TGFBR1 protein and 14B-octamethyl-1 compound with a docking score of –11.4 kcal/mol, which acts as a promising compound against skin cancer.

1. Introduction

Rosemary (*Salvia rosmarinus* Spenn.) belongs to the Lamiaceae family and is widely explored for its medicinal properties among the genus *Salvia* (Paviæ *et al*., 2019). It is an evergreen perennial shrub, cultivated and is native to the Mediterranean region. The five-foot perennial shrub is frequently used in sauce, food preservatives, cooking, and other products; in addition, it is also used in the cosmetic and therapeutic industries (Nguyen *et al*., 2021). In folk medicine, rosemary is used to heal wounds, treat inflammatory illnesses and mycoses, as well as to treat renal colic, muscle spasms, dysmenorrhea, and headaches (Borella *et al*., 2019; de Macedo *et al*., 2020).

Rosemary, the major source of carnosic acid, is widely recognised for its biological effects, such as its anti-inflammatory, antioxidant, and neuroprotective properties. The catechol moiety gives the molecule strong antioxidant properties, while the terpene skeleton makes it fat-soluble. Carnosic acid (CA), a phenolic diterpene, belongs to the terpenoids, isoprenoids, or terpenes class of secondary plant metabolites (Hill and Connolly, 2017). Carnosic acid content in dried rosemary or sage leaves can range from 0.1% to 7%, depending on the species, variety, and environmental factors that affect plant growth, as well as sample preparation and extraction methods. More than 90% of the antioxidant properties of rosemary extract are thought to be attributed to carnosic acid (Paviæ *et al*., 2019). High yield purity and reproducibility are key components of the separation process. To create environment-friendly green solvents and to identify the high-yield extraction method (Sivakumar *et al*., 2022; Chemat *et al*., 2019). Several methods, including the use of ethanol as an organic solvent, are used to extract carnosic acid. The most popular methods for extracting CA include Maceration, Soxhlet, and Ultrasonication. Maceration has been the most widely used and cost-effective technique for producing bioactive chemicals. Even though, this process is simple and may be completed in a day at room temperature (Bernatoniene *et al*., 2016), Soxhlet extraction is a time- and labour-intensive process. Using the Soxhlet method, valuable bioactives have been extracted from plant sources (Caleja *et al*., 2017). Ultrasonication-assisted extraction is a good substitute for traditional extraction techniques because it has higher extraction efficiency by using ultrasonic energy to damage the cellular structures of the plant materials, and CA is extracted in just 30 min (Fomo *et al*., 2020).

DNA barcoding, a widely used technique for species identification, leverages conserved genomic regions to build extensive reference libraries. Examining short, standardised DNA sequences instead of full genomes enables rapid and accurate species identification, facilitating studies in ecology, agriculture, water quality, conservation, and medicinal plant identification. The high-throughput approach of gathering complete DNA barcodes is often slow and resource-intensive and instead favours sequencing short, standardised regions of the DNA (El-Atroush, 2020). Moreover, DNA barcoding with internal transcribed spacers (ITS) and matK enables massive-scale species identification and DNA fingerprints for virtually every species on

Corresponding author: Dr. S. Tamilselvi
Professor, Department of Biotechnology, Bannari Amman Institute of Technology, Sathyamangalam-638401, Erode, Tamil Nadu, India
E-mail: tamilselvis@bitsathy.ac.in
Tel.: +91-9942588072

earth. Barcoding is extremely important in the areas of biodiversity conservation efforts as well (Sarvananda, 2018). Plants' barcodes, ITS, and matK, which exhibit high copy number amplification due to other genes' existence, are located in another genome (Shafqat *et al.,* 2018; Masi Malaiyan *et al*., 2023).

The skin, our largest organ, acts as a protective barrier against environmental hazards. However, skin cancer is increasingly prevalent, influenced by viral infections, genetic mutations, and environmental factors. Cancer can originate in various skin cell types, and new treatments are needed to enhance the prognosis. Research into medicinal plants shows promise for inhibiting skin cancer cell proliferation (Suganthi and Malarvizhi, 2020; Penta *et al*., 2018). Transforming growth factor beta (TGF-β) plays a dual role in cancer as both a tumour suppressor and promoter of invasion by modulating immune responses (Xue *et al*., 2020). SB431542, an inhibitor of TGF-β type I receptors ALK4, ALK5, and ALK7, has shown potential in targeting TGF-β signalling pathways in cancer progression (Teicher, 2021).

The present study aimed to validate the extraction of carnosic acid using various extraction techniques and to authenticate the plant sample using DNA barcoding in *S. rosmarinus* and molecular docking studies to explain the specific ligand compound and target protein prediction.

2. Materials and Methods

2.1 Plant collection and sample preparation

The plant sample was collected from the Kadambur region and authenticated as *Salvia rosmarinus* Spenn. from the Botanical Survey of India, Tamil Nadu Agricultural University, Coimbatore, with the authentication number BSI/SRC/5/23/2024-25/Tech/495. The dried leaves were ground into a fine powder for subsequent validation of carnosic acid content in the ethanolic leaf extract of rosemary.

2.2 PCR and gene sequencing

DNA barcoding was performed using the ITS gene, which was amplified by PCR. The amplified products were sent to the Rajiv Gandhi Centre for Biotechnology, Trivandrum, Kerala, for sequencing. The ITS sequences were analysed using the NCBI Basic Local Alignment Tool (BLAST) tool for species identification.

The most commonly employed docking tools are AutoDock Vina and PYRX (Pawar *et al*., 2021). Docking predicts the binding site of protein on attachment of ligand; the ligand must be in a six-dimensional rotational or translational space (Rohane and Makwana, 2019). Chemical probes are found and created using a library of chemical probes using high-throughput tiny-molecule screening.

2.3 Sequence alignment and data analysis

S. rosmarinus DNA was barcoded using the BLAST. Sequences with low quantity and ambiguity were manually inspected and eliminated. The NCBI database has 99 ITS sequences in total, which were compared. The query sequences were found using the maximum hits (99 or 100%) with a species in the reference database and the E value of 1*10-5 (Surya and Hari, 2017).

2.4. Phylogenetic analysis

The sequence datasets were analysed using neighbour-joining (NJ) techniques. Using MEGA version 6.06, the NJ tree was built using the distance substitution-based K2P model. 1000 replicates were used to estimate the bootstrap support for the NJ tree, and any unhelpful characters (gaps and missing data) were completely removed (Ahmed, 2019).

2.5 Methods of extraction

Traditional extraction techniques including Maceration, Soxhlet extraction, and Ultrasound extraction were used in our study. The 2 g dried and powdered sample was combined with 40 ml of 99% ethanol (1:5) and left to set overnight. The overnight filter is referred to as the maceration extraction. The rosemary sample was wrapped in filter paper before being added to the soxhlet apparatus. Following the completion of the three-cycle procedure, the rosemary extract was taken. The rosemary sample was again collected for ultrasound extraction and held at 140 mW for 50 min (Kumar *et al.,* 2023).

After extraction, the filter is extracted and added 5% sodium bicarbonate ($NaHCO_3$) to one-third of the extract and then filtered. After collecting the aqueous layers, then 2 M HCl was added to the solution to adjust the pH 2. After that, it is re-extracted with hexane, passed through cheesecloth, and then dried.

2.6 GC-MS analysis

Gas chromatography-mass spectrometry (GC-MS) is a scientific procedure that combines the best aspects of gas chromatography and mass spectrometry to identify various substances in a test. Helium was used as the carrier gas during the analysis, and a continuous flow rate of 1 ml/min was employed to separate the components using a fused silica column filled with Elite-5MS (5% biphenyl, 95% dimethylpolysiloxane, 30 m 0.25 mm ID, 250 mm df). During the chromatographic run, the injector temperature was set to 2600°C. The oven temperature was set to the following when the 1 l of extract sample was injected into the apparatus: It was held at 600°C for two minutes and then increased to 3000°C at a rate of 100°C/ min. The conditions for the mass detector were as follows: a scan time of 0.2 sec, a scanning interval of 0.1 sec, a transfer line temperature of 2300°C, an ion source temperature of 2300°C, and an electron impact in the ionisation mode of 70 eV. fragments between 40 and 600 Da. The component spectra were compared to a database of known component spectra kept in the GC-MS NIST (2008) library (Aamer *et al.*, 2023).

2.7 FT-IR analysis

The different functional groups present in the sample can be identified through FTIR analysis. The dried sample was further ground into a fine powder. A small amount of pressure was added along with the test and KBr. In the chemistry lab at the Bannari Amman Institute of Technology (BIT), Sathyamangalam, Erode, the powder was formed into a pellet and analysed for FTIR (Shimadzu) at a range of 400 to 4000 cm^{-1} (Al-Bayati, 2011).

2.8 HPLC analysis

High-performance liquid chromatography (HPLC), with an Agilent 1220, was used at the Bannari Amman Institute of Technology (BIT), Sathyamangalam, Erode, to analyse carnosic acid. The amount of carnosic acid was measured using an HPLC system with a UV detector with a scanning range of 285 nm and a reversed-phase C18 column of 4.6100 mm. For the molecule elution, two phases were employed: the mobile phase (A) consisted of HPLC-grade methanol (Sigma-

Aldrich), and the mobile phase (B) was MilliQ water containing 0.1% formic acid. Before being injected (2 l) into the mobile phase at a flow rate of 0.4 ml/min, the sample was filtered through a 0.45 m membrane. Carnosic acid in HPLC had a 15 min retention time (Yeddes *et al.,* 2022).

2.9 Antioxidant assay

The antioxidant activity was measured with the DPPH (2,2 diphenyl-1-picrylhydrazine hydrate) assay, which was more specific to the DPPH radical than other radicals. The different concentrations (50-250 µg/ml) of the 0.1 mM DPPH were added. After vigorously shaking the mixture, the tubes were tightly sealed and left to stand for 30 min in the dark. At 517 nm, absorbance was measured against blank samples and compared to the ascorbic acid calibration curve. The percentage of DPPH radical inhibition was calculated using the formula below (Sameemabegum *et al*., 2022).

$$\% \text{ of inhibition} = (A_0 - A_1/A_0) \times 100$$

Where A_0 represents the absorbance of the reference reaction. A_1 is the test compound absorbance, and the IC_{50} value is the number of antioxidants required in total to reduce the initial DPPH concentration by 50% (Harba *et al.,* 2021).

2.10 Ligand preparation

The PubChem database was searched to find the chemical structures of the twelve compounds. The compound CID numbers and the canonical SMILE notation were noted, and the ligand was downloaded in sdf format (Daina *et al.,* 2017).

2.11 *In silico* pharmacokinetic analysis

The energy-minimised ligands were examined pharmacokinetically, which include absorption, distribution, metabolism, and excretion. The Swiss ADME server was used for the analysis. One by one, the canonical grins were pasted onto the Swiss ADME server. The substance was thought to possess several ADME-related qualities, such as blood-brain barrier penetration, gastrointestinal absorption, phosphoglycerate substrate, Logkp, LogPo/w, LogS, cytochrome 450 substrate or inhibitor, carcinogenicity, cytotoxicity, hepatotoxicity, immunotoxicity, and mutagenicity. ADME testing assists in defining promising compounds to distinguish between those that have significant disqualifying flaws and those that have potential as pharmacological compounds (Banerjee *et al.,* 2018).

2.12 Protein retrieval and preparation

The TGFBR1 protein was identified through a search of the Protein Data Bank (PDB) database. Before docking, PyRx was used to remove the solvent and additional bound organic and inorganic moieties from the protein. Using PyRx software, polar hydrogen was added to the protein after water molecules were eliminated from the protein-ligand docking process. To run Auto Dock Vina, the protein's PDB format was finally converted to pdbqt format (Abbas *et al.,* 2023).

2.13 Docking analysis

Interactions between ligands and proteins are determined by binding affinity. The docking score is identified by the bioinformatics tool, AutoDock Vina. It uses the Lamarckian genetic algorithm and empirical free energy scoring function to produce a typically reproducible docking result. The grid spacing was 0.375 Å inches. 70 × 70 × 70 (x, y, and z) points were chosen as the grid dimensions, with x, y, and z acting as the grid x, y, and z centers, respectively. The estimated free energy of binding was used to evaluate the efficacy of compounds docking against the enzyme (Tian *et al.,* 2018).

3. Results

The samples were sequenced at the Rajiv Gandhi Centre for Biotechnology, Trivandrum, Kerala. The ITS sequences were analysed using the NCBI BLAST tool for species identification.

3.1 Sequence alignment and data analysis

The phylogenetic tree analysis and BLAST data of matching results for *S. rosmarinus* are displayed in Table 1 and Figure 1. The most similar plant species are represented, with the highest percentages. The ITS sequence served as a barcode. ITS sequence alignments against GenBank accessions produced query coverages ranging from 90 to 98% and 89%, respectively. Based on sequence alignment analysis, 99% of the *S. rosmarinus* genus length was found for ITS.

Table 1: Degree of similarity between the query sequence and hits

S.No.	Genus	Species	Alignment Score	Similarity (%)
1	*Salvia*	*S. rosmarinus*	1107	98.72
2	*Salvia*	*S. yangii*	911	91.29
3	*Salvia*	*S. henryi*	979	91.03
4	*Salvia*	*S. dorystaechas*	965	90.64
5	*Salvia*	*S. dolomitica*	952	90.41
6	*Salvia*	*S. sessilifolia*	953	90.42
7	*Salvia*	*S. texana*	952	90.45
8	*Salvia*	*S. whitehousei*	950	90.35
9	*Salvia*	*S. summa*	998	91.43
10	*Salvia*	*S. pentstemo noides*	957	90.39
11	*Salvia*	*S. scrophul ariifolia*	1038	92.18
12	*Salvia*	*S. rugosa*	970	90.54
13	*Salvia*	*S. rosmarinus*	1040	97.83
14	*Salvia*	*S. rosmarinus*	1050	96.96
15	*Salvia*	*S. rosmarinus*	1201	98.95
16	*Salvia*	*S. rosmarinus*	1212	98.68
17	*Salvia*	*S. rosmarinus*	1116	96.12
18	*Salvia*	*S. davidsonii*	920	90.70
19	*Salvia*	*S. rosmarinus*	1463	98.90
20	*Salvia*	*S. officinalis*	1094	90.72
21	*Melissa*	*M. officinalis*	1090	90.82

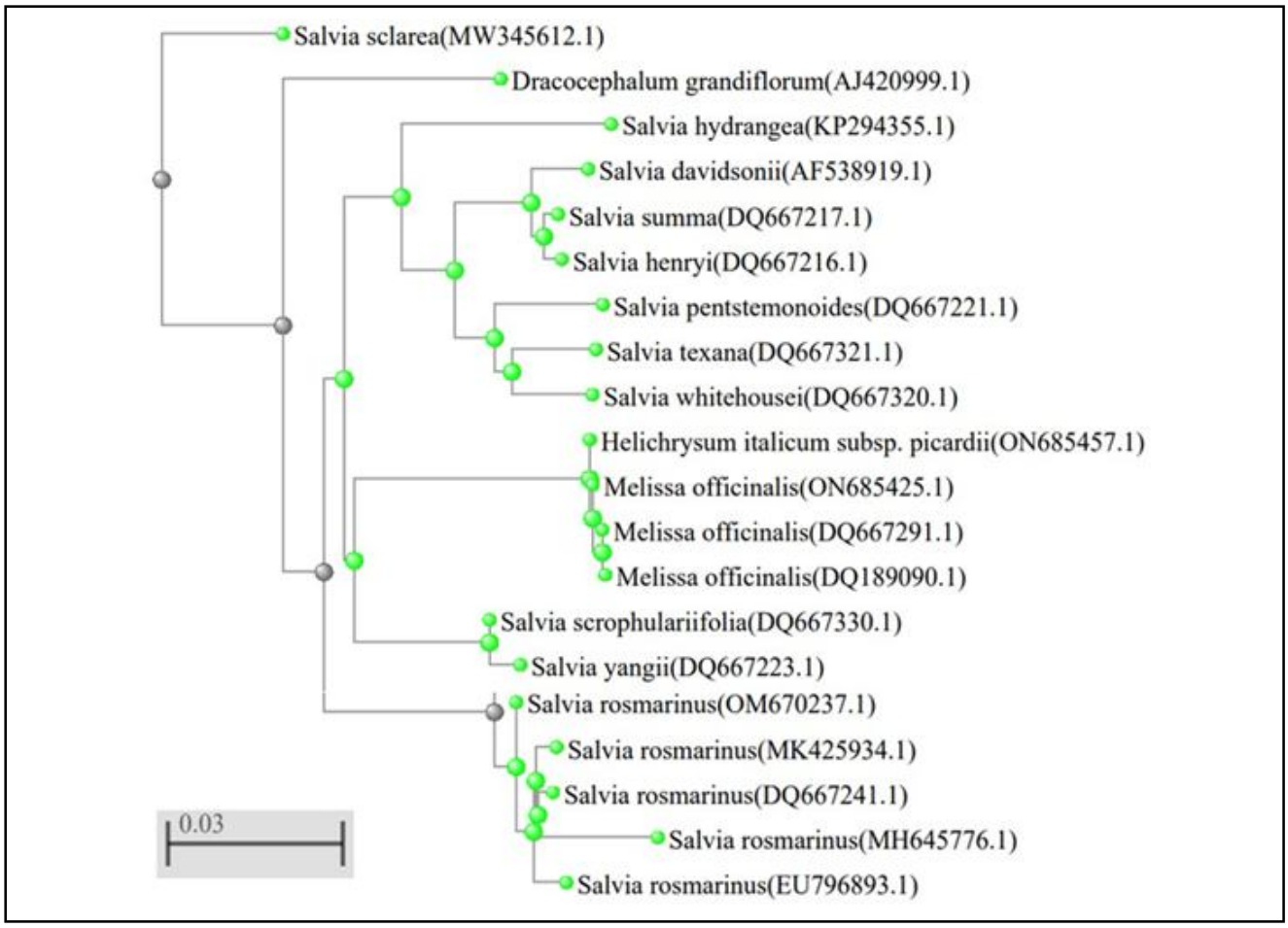

Figure 1: Phylogenetic tree of *S. rosmarinus* nuclear marker and ITS gene.3.2. Phylogenetic tree families and clustering

The maximum composite likelihood method was utilised to compute the evolutionary distances, while the neighbour-joining method was employed to construct the phylogenetic tree. The current study displays the evolutionary relationships among the medicinal species of *S. rosmarinus*. The phylogenetic tree of the plant species with the highest similarity percentages (Figure 1) illustrates how closely related species are clustered together and how relatively distant species are distributed.

3.3 Extraction of carnosic acid from *S. rosmarinus*

Carnosic acid extraction from *S. rosmarinus* leaf using maceration, soxhlet, and ultrasound methods. The yield of carnosic acid using various ethanolic extract validation methods has been measured using three different extraction techniques. From the study, one of the more effective extraction methods and yields are shown in Figure 2.

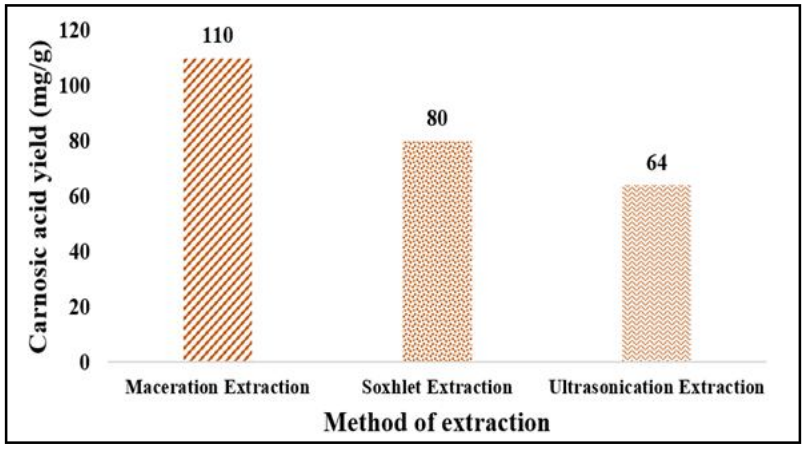

Figure 2: Yield of carnosic acid by using different extraction methods.

3.4 GC-MS analysis

Chromatogram for ethanolic extraction of carnosic acid is shown in Figure 3. The samples were analysed quantitatively in the Vellore Institute of Technology-Sophisticated Instrument Facility Laboratory. Table 2 lists the findings from the GC-MS analysis of the ethanolic extract of *S. rosmarinus* leaf, such as, 3-octen-5-yne, 2,7- dimethyl-, (E) (7.92), 1,3,6-heptatriene, 2,5,5-trimethyl ros (2.56), 4-carene (1.55), eucalyptol (24.6), 2-heptanol, 4-methyl (3.371), 1-dodecyne (6.008), camphor (10.84), 1-tetradecyne (4.456), 1-tetradecyne (2.38), bicyclo (2.2.1) heptan-2-one, 1, 7, 7-trimethyl-, (+/-) (2.44), 3-cyclohexyldimethy siloxy-tetradecane (2.103), 14b-octamethyl-1 (7.173), dihydro-cis-alpha-copaene-8-ol (12.10). Figure 3 shows the compound retention time in the GC-MS analysis.

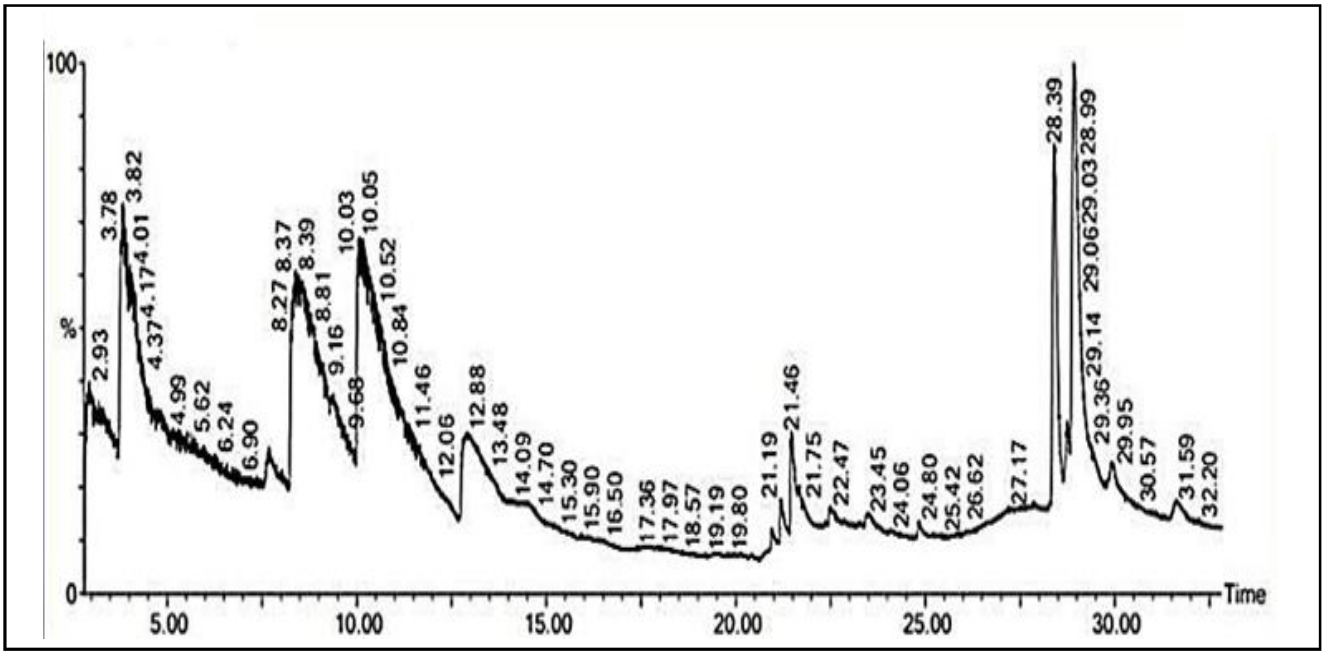

Figure 3: GC-MS chromatogram of ethanolic leaf extract of *S. rosmarinus*.

Table 2: Bioactive compounds detected from ethanol extract of *S. rosmarinus*

S.No.	Retention time	Area%	Molecular weight(g/mol)	Compounds
1	3.819	7.922	136	3-Octen-5-Yne,2,7-Dimethyl-,(E)-
2	4.109	2.562	136	1,3,6-Heptatriene, 2,5,5-Trimethylros-
3	4.279	1.550	136	4-Carene
4	8.386	24.675	154	Eucalyptol
5	9.381	3.371	130	2-Heptanol,4-Methyl
6	10.106	6.008	166	1-Dodecyne
7	10.191	10.848	152	Camphor
8	10.607	4.456	194	1-Tetradecyne
9	10.887	2.385	152	1-Tetradecyne
10	11.112	2.446	152	Bicyclo[2.2.1]Heptan-2-One,1,7,7-Trimethyl-, (+/-)-
11	21.461	2.103	354	3- Cyclohexyl dimethysiloxy-Tetradecane
12	28.389	7.173	424	14b-Octamethyl-1
13	28.909	12.107	222	Dihydro-Cis-Alpha-Copaene-8-Ol

3.5 FTIR analysis

The FTIR spectrum depicts the band at the peaks and lists the functional groups (Table 3). The suitable method for identifying any functional group is FTIR spectroscopy (400-4000 cm^{-1}) and the characteristic bands that are detected, in that order. 3423 stretching vibrations at (OH), 2654 stretching vibrations (C-H, C=H), 2931 stretching vibrations (COO-H), and 1693 stretching vibrations (C=O) were found to be in a broadband.

3.6. HPLC analysis

The HPLC analysis of the carnosic acid extraction is shown in Figure 4, where the following peaks are visible. The retention times for the carnosic acid and standard were found to be 6.189 and 5.962 min, respectively (Table 4). Carnosic acid, obtained from *S. rosmarinus*, is detected by HPLC (de A Cavalcante *et al.,* 2022). Carnosic acid has a retention time of 5.962 min in the standard HPLC profile (Figure 4), and carnosic acid runs at a retention time of 6.189 min in the sample HPLC profile (Fatma Ebru *et al.,* 2017).

Table 3: FTIR spectral peak values and functional groups obtained for the carnosic acid from *S. rosmarinus*

S.No.	Wave number (cm^{-1})	Functional group
1	3423.65	Phenolic group
2	2931.80	Alkanes
3	2654.05	Carboxylic acid
4	1693.50	Amide
5	1458.18	Alkenes group
6	1246.02	Aliphatic amine
7	887.26	Aromatics

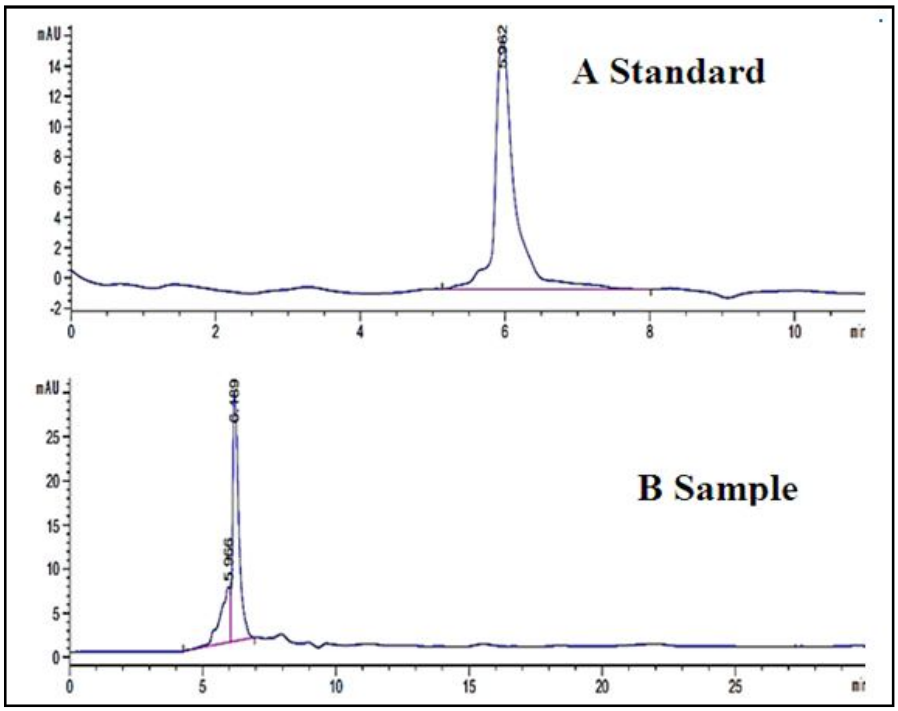

Figure 4: HPLC chromatogram for carnosic acid.

Table 4: HPLC chromatogram of carnosic acid retention time for standard and sample

Peak #	Rt time (min)	Width (min)	Area (mAU*s)	Height (mAU)	Area %
1	6.189	0.4113	1.3772	6617.607	0.7830
2	8.135	0.8654	1.6381	2.40025	93.1279
3	9.477	0.5978	3.0214	816.874	0.1718
4	10.692	0.5473	1.2293	3313.572	0.6989
5	11.561	0.2749	7422.44	425.276	0.0422
6	12.179	0.4552	1.5272	516.434	0.0868
7	5.962	0.2764	319.310	16.5999	100.000

3.7 Antioxidant activity

As seen in Figure 5, these findings suggest that during carnosic acid's antioxidant process, free radicals are created. Figure 5 displays the DPPH of RSA%, and a study produced an IC_{50} value of 12.87 µg/ml.

3.8. *In silico* pharmacokinetic assessment

The Swiss ADME software consists of data on drug likeliness, pharmacokinetics, physiochemical properties, lipophilicity, water solubility, and medicinal chemistry. The results are shown in Tables 5 and 6.

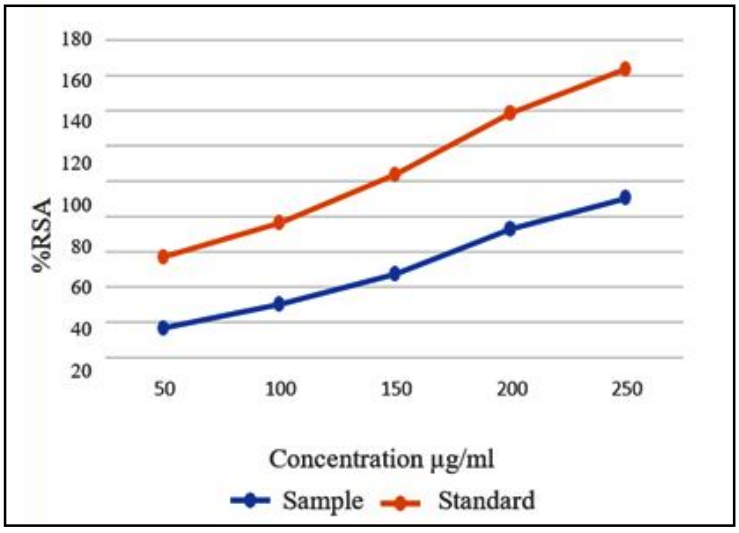

Figure 5: Antioxidant activity of carnosic acid.

Table 5: Swiss ADME analysis of ligands

S. No.	Compounds	MW (g/mol)	H- Bond donor	H-bond acceptor	Lipophilicity Log $p_{o/w}$ (MLOGP)	Drug likeness
1	3-Octen-5-yne, 2,7-dimethyl-,(e)	136.23	0	0	4.57	1
2	4 Carene	136.23	0	0	4.29	1
3	Eucalyptol	154.25	0	1	2.45	0
4	2-Heptanol, 4-Methyl	175.23	1	3	0.70	0
5	1-Dodecyne	190.21	0	4	0.74	0
6	1-Tetradecyne	194.26	0	0	3.70	1
7	Bycyclo [2.2.1]Heptan-2-One,1,7,7-Trimethyl-,(+/-)	240.34	0	1	3.78	0
8	14b-Octamethyl-1	426.72	1	1	4.73	1
9	Dihydro-Cis-Alpha-Copaene-8-Ol	222.37	1	1	3.81	0

Table 6: Admet SAR analysis for ligands

S.No.	Compounds	Ames toxicity	Carcinogens	Acute oral toxicity	Rat acute toxicity LD_{50}, (mol/kg)
1	3-Octen-5-Yne, 2,7-Dimethyl-,(E)-	Non-AMES	Carcinogen	III	1.8438
2	4carene	Non-AMES	Non-Carcinogen	III	1.6324
3	Eucalyptol	Non-AMES	Non-Carcinogen	III	1.8144
4	2-Heptanol,4-Methyl	Non-AMES	Carcinogen	III	2.3092
5	1-Dodecyne	AMES	Carcinogen	I	3.7207
6	1-Tetradecyne	Non-AMES	Carcinogen	III	1.6636
7	Bycyclo[2.2.1]Heptan-2-One,1,7,7-Trimethyl-, (+/-)-	Non-AMES	Carcinogen	III	1.8675
8	14 b-Octamethyl-1	Non-AMES	Non-Carcinogen	III	2.0842
9	Dihydro-Cis-Alpha-Copaene-8-Ol	Non-AMES	Non-Carcinogen	III	2.2468

Using *in silico* screening techniques, the pharmacokinetic characteristics of compounds are examined. Swiss ADME predictions were utilized to analyze the drug-like properties of the synthesised compounds during this work. To evaluate the compounds' toxicity and carcinogenic potential, an ADME analysis was carried out. Absorption, distribution, metabolism, and excretion (ADME) qualities are important considerations in the creation of medications (Riyadi *et al*., 2021). The Lipinski rule of five was applied to the analysis of the data. These substances meet Lipinski's criteria for drugs by having adequate ADME properties. The analysis states that for molecules that meet two or more of the following rules, there is a high likelihood of success or failure because of drug-likeness. Less than five hydrogen bond donors, less than ten hydrogen bond acceptors, a molecular mass of less than 500 Dalton, high lipophilicity (represented as log P less than 5), and a molar refractivity of between 40 and 130 are all desirable (Teicher, 2021; Pawar *et al.,* 2021).

3.9 Molecular docking analysis

For docking analysis, the three-dimensional crystal structure of TGFBR1 (PDB ID: "1PY5") was obtained from the protein data bank. The PubChem database was used to obtain the *S. rosmarinus* leaf extract's 13 active compounds (SDF). Using the PyRx AutoDock Vina tool, the hit ligand or active compounds were screened against the target TGFBR1.

Out of the thirteen compounds, nine were identified as follows: 3-octen-5-yne, 2,7-dimethyl, (E), 4-carene, eucalyptol, 2-heptanol, 4-methyl, 1-dodecyne, 1-tetradecyne, bicycloHeptan-2-ol, 1, 7, 7-trimethyl-, (+/-), 14b-octamethyl-1, dihydro-cis-alpha-copaene-8-ol with docking scores of -5.7, -6.2, -2.5, -5.4, -2.6, -8.1, and -3.1, respectively. The standard compound is 4-(4-(benzo[D] [1,3] dioxol-5-yl)-5-(pyridin-2-yl)-1h-imidazol-2-yl) benzamide, which is the compound inhibitor SB431542 that had a docking score of -11.4 kcal/mol. In contrast to the nine compounds 4-(4-(benzo[D] [1,3] dioxol-5-yl)-5-(pyridin-2-Yl)-1h-imidazol-2-yl), benzamide and 14b-octamethyl-1 displayed favourable docking outcomes (Figure 6).

3.10 Protein-ligand interaction analysis

The hydrophobic interaction and hydrogen bonds between the ligand and the protein's amino acids have been emphasised using protein-ligand analysis. Predicting the ligand-target protein binding affinity is made easier by docking tools. Figure 7 shows the schematic 2D representation of the interaction between the ligands and the target protein.

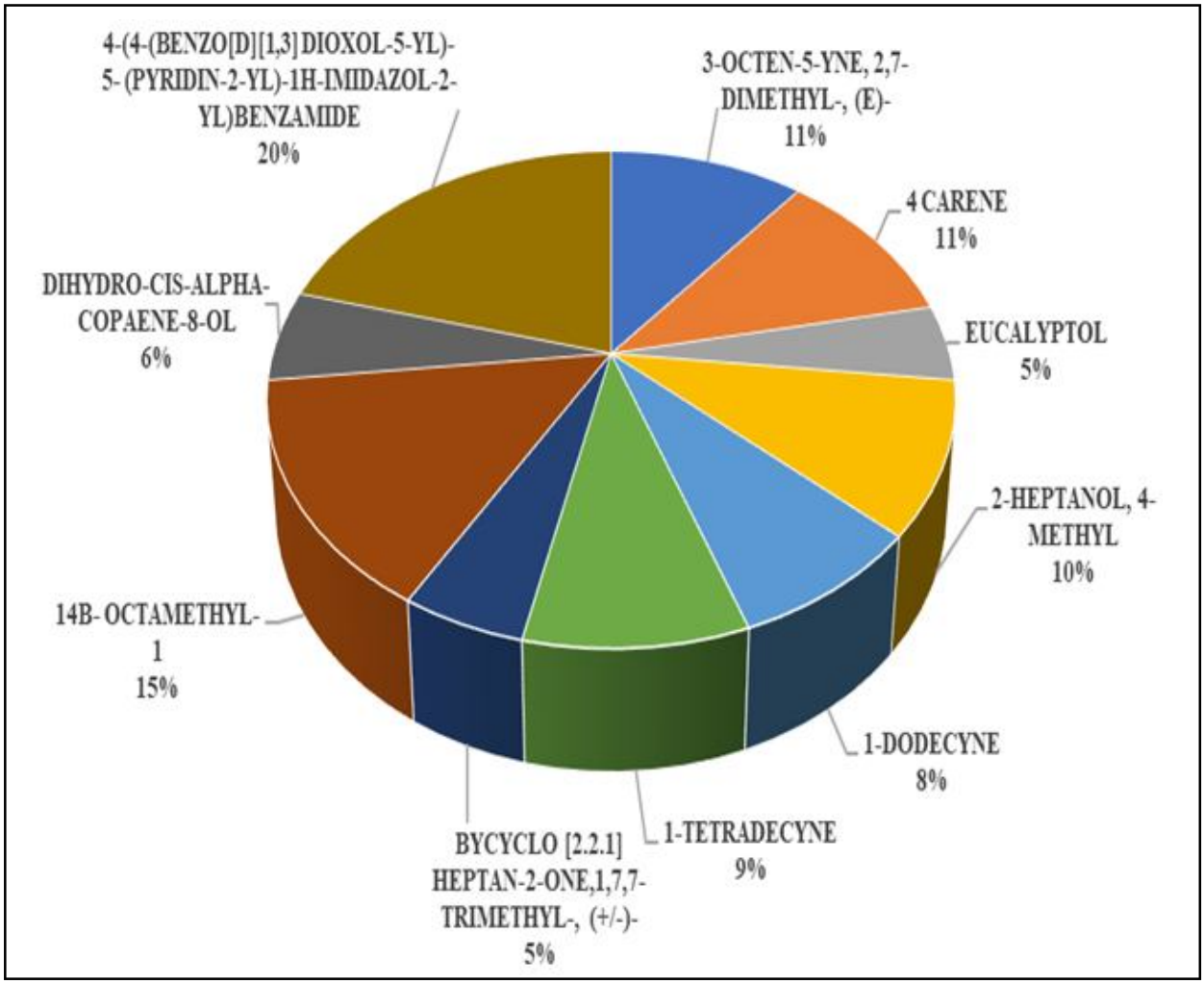

Figure 6: Docking score analyzed by AutoDock Vina.

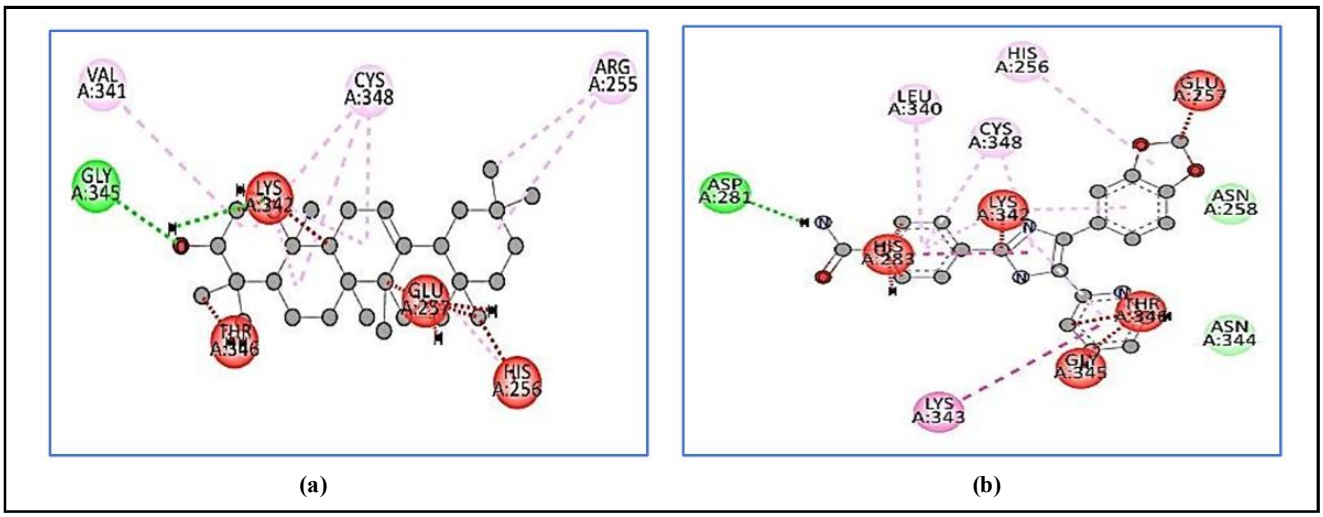

Figure 7: (a)- Binding interaction of 14B- octamethyl-1 with TGFBR1 protein; (b)- Binding interaction of 4-(4-(benzo[D] [1,3] dioxol-5-yl)-5-(pyridin-2-Yl)-1h-Imidazol-2 yl) Benzamide interaction with TGFBR1protein.

4. Discussion

Carnosic acid holds significant therapeutic properties and is widely explored in the cosmetic and pharmaceutical industries. DNA barcoding, specifically the internal transcribed spacer region, is utilised for the identification of accurate species to ensure the authenticity of rosemary-derived products. Building a neighbor-joining phylogenetic tree is made possible by successful PCR amplification that confirmed a 99% match with *S. rosmarinus* using BLAST. Lipinski's Rule is followed to test the ADME properties of compounds. The extraction of the target carnosic acid under various operating conditions like Maceration extraction, Soxhlet extraction, and Ultrasound extraction was reported to have a higher yield of 110 mg from maceration extraction as compared to the other two methods. Thirteen compounds were identified by ethanolic extract by GC-MS analytical technique, exhibiting unique retention times corresponding to molecular weight and peak areas. Functional groups in carnosic acid are confirmed by FTIR analysis, which revealed its antioxidant properties. Molecular docking, widely used in drug discovery, structurally illustrated the binding interactions between compounds and the TGFBR1 protein, strongly representing hydrophobic bonds. Promising binding energy with potent interactions is exhibited by the compound 14B-octamethyl-1 with a docking score of -11.4 kcal/mol for skin cancer therapy. Similarly, Demir *et al*. (2024) studied the effect of carnosic acid against the enzymes 6PGD and G6PD involved in the pentose phosphate pathway and concluded the binding score to be -7.8 kcal/mol and -7.4 kcal/mol, respectively. The docking score confirmed the binding affinity between compounds and proteins, highlighting the therapeutic properties of carnosic acid, especially for cancer treatment. The study showcased the importance of *S. rosmarinus* in the therapeutic field against GFBR1, a cancer-inducing oncogene for skin cancer. Highlighting the importance of carnosic acid against skin cancer using *in silico* studies, this study can be further explored using animal studies.

5. Conclusion

The study discovered that the ITS region is highly effective for DNA barcoding of plant groups and is one of the most important tools for verifying the identity of known species. Maceration is reported to be the most effective method of extraction of carnosic acid using ethanol. The chemical compounds characterised from the extracts using GC-MS, FTIR, and HPLC analyses were reported to have free radical scavenging activity. Also, the compounds act as ligands and neutralise the activity of the enzyme transforming growth factor beta receptor type-I kinase (TGFBR1), which is the target protein against skin cancer in targeted drug therapy. The pharmacokinetic analysis, drug likeliness, and binding affinity supported the targeted binding of the ligand with the enzyme. As per the findings, the study concludes the secondary metabolite carnosic acid extracted from rosemary is an efficient drug against the skin cancer-inducing enzyme.

Conflict of interest

The authors declare no conflict of interest relevant to this article.

References

Aamer, H. A.; Al-Askar, A. A.; Gaber, M. A.; El-Tanbouly, R.; Abdelkhalek, A.; Behiry, S. and El-Messeiry, S. (2023). Extraction, phytochemical characterization, and antifungal activity of *Salvia rosmarinus* Spenn. extract. Open Chemistry, **21**(1):20230124.

Abbas, K.; Alam, M.; Ali, V. and Ajaz, M. (2023). Virtual screening, molecular docking and ADME/T properties analysis of neuroprotective property present in root extract of chinese skullcap against β-site amyloid precursor protein cleaving enzyme 1 (BACE1) in case of Alzheimer's disease. Journal of Pharmacognosy and Phytochemistry, **12**(1):146-153.

Ahmed, S.M. (2019). Phylogenetic analysis of *Rosa damascena* L. from Taif using DNA barcoding approach. Pak. J. Bot, **51**(1):157-164.

Al-Bayati, F. A. (2011). Antimicrobial activity of carnosic acid isolated from *Rosmarinus officinalis* L. leaves. Tikrit J. Pure Sci., **16**:1662-1813.

Banerjee, P.; Eckert, A. O.; Schrey, A. K. and Preissner, R. (2018). ProTox-II: A webserver for the prediction of toxicity of chemicals. Nucleic Acids Research, **46**(W1):W257-W263.

Bernatoniene, J.; Cizauskaite, U.; Ivanauskas, L.; Jakstas, V.; Kalveniene, Z. and Kopustinskiene, D. M. (2016). Novel approaches to optimize extraction processes of ursolic, oleanolic and rosmarinic acids from *Rosmarinus officinalis* leaves. Industrial Crops and Products, **84**:72-79.

Brindisi, M.;Bouzidi, C.; Frattaruolo, L.;Loizzo, M. R.; Tundis, R.; Dugay, A. and Cappello, M. S. (2020). Chemical profile, antioxidant, anti-inflammatory, and anticancer effects of Italian *Salvia rosmarinus* Spenn. methanol leaves extracts. Antioxidants, **9**(9):826.

Caleja, C.; Barros, L.; Prieto, M. A.; Barreiro, M. F.; Oliveira, M. B. P. and Ferreira, I. C. (2017). Extraction of rosmarinic acid from *Melissa officinalis* L. by heat, microwave-and ultrasound-assisted extraction techniques: A comparative study through response surface analysis. Separation and Purification Technology, **186**:297-308.

Chemat, F.; Abert-Vian, M.; Fabiano-Tixier, A. S.; Strube, J.; Uhlenbrock, L.; Gunjevic, V. and Cravotto, G. (2019). Green extraction of natural products. Origins, current status, and future challenges. Trends in Analytical Chemistry, **118**:248-263.

Daina, A.; Michielin, O. and Zoete, V. (2017). Swiss ADME: A free web tool to evaluate pharmacokinetics, drug-likeness, and medicinal chemistry friendliness of small molecules. Scientific Reports, **7**(1):42717.

De A Cavalcante, M.; dos S Oliveira, J.; da S Barreto, M. S.; Pinheiro, L. P.; de C Cantuária, P.; Borges, W. L. and de Souza, T. M. (2022). An hplc method to determine phenolic compounds of plant extracts: Application to *Byrsonima crassifolia* and *Senna alata* leaves. Pharmacognosy Research, **14**(4):395-404.

De Macedo, L. M.; Santos, E. M. D.; Militao, L.; Tundisi, L. L.; Ataide, J. A.; Souto, E. B. and Mazzola, P. G. (2020). Rosemary (*Rosmarinus officinalis* L., *Salvia rosmarinus* Spenn.) and its topical applications: A review. Plants, **9**(5):651.

Demir, Y.; Öztürk, N.; Isýyel, M. and Ceylan, H. (2024). Effects of carnosic and usnic acid on pentose phosphate pathway enzymes: An experimental and molecular docking study. Chemistry Select, **9**(27):e202401067.

El-Atroush, H. (2020). DNA barcoding of two medicinal plants using molecular markers. Egyptian Academic Journal of Biological Sciences. C, Physiology and Molecular Biology, **12**(1):83-92.

Fatma Ebru, K.; Ayse, A. and Caglar, K. (2017). Extraction and HPLC analysis of sage (*Salvia officinalis*) plant. Nat. Prod. Chem. Res., **5**(8):8-10.

Fomo, G.; Madzimbamuto, T. N. and Ojumu, T. V. (2020). Applications of nonconventional green extraction technologies in process industries: Challenges, limitations and perspectives. Sustainability, **12**(13):5244.

Harba, Y. A. H. A.; Fadal, S. A. M. A. and Noor, U. M. (2021). Study of antioxidant, biological activity and docking study for phenolic acids in *Rosmarinus officinalis* l. Crude extract. Plant Archives, **21**(1):0972 5210.

Hill, R. A. and Connolly, J. D. (2017). Triterpenoids. Natural Product Reports, **34**(1):90-122.

Masi Malaiyan, M.; Mohan Kumar, P.; Logesh, P.; Sibi, K.; Tamizharasi, S.; Nandhakumaran, J.; Janani S. and Prabha T. (2023). Discovering the epigenetic pathways underlying SARS-COV-2 infections and exploring recent epigenetic-associated clinical trials. Ann. Phytomed., **12**(2):12-20.

Nguyen, H. C.; Nguyen, H. N. T.; Huang, M. Y.; Lin, K. H.; Pham, D. C.; Tran, Y. B. and Su, C. H. (2021). Optimization of aqueous enzyme assisted extraction of rosmarinic acid from rosemary (*Rosmarinus officinalis* L.) leaves and the antioxidant activity of the extract. Journal of Food Processing and Preservation, **45**(3):e15221.

Pavic, V.; Jakovljevic, M.; Molnar, M. and Jokic, S. (2019). Extraction of carnosic acid and carnosol from sage (*Salvia officinalis* L.) leaves by supercritical fluid extraction and their antioxidant and antibacterial activity. Plants, **8**(1):16.

Pawar, R. P. and Rohane, S. H. (2021). Role of autodockvina in PyRx molecular docking. Asian J. Research Chem., **14**(2*):1*32-134.

Penta, D.; Somashekar, B. S. and Meeran, S. M. (2018). Epigenetics of skin cancer: Interventions by selected bioactive phytochemicals. Photodermatology, Photoimmunology and Photomedicine, **34**(1):42-49.

Rahbardar, M. G.; Amin, B.; Mehri, S.; Mirnajafi-Zadeh, S. J. and Hosseinzadeh, H. (2017). Anti-inflammatory effects of ethanolic extract of *Rosmarinus officinalis* L. and rosmarinic acid in a rat model of neuropathic pain. Biomedicine and Pharmacotherapy, **86**:441-449.

Riyadi, P. H.; Sari, I. D.; Kurniasih, R. A.; Agustini, T. W.; Swastawati, F.; Herawati, V. E. and Tanod, W. A. (2021). Swiss ADME predictions of pharmacokinetics and drug-likeness properties of small molecules present in *Spirulina platensis*. In IOP conference series: earth and environmental science. IOP Publishing, **890**(1):012021.

Rohane, S. H. and Makwana, A. G. (2019). In silico study for the prediction of multiple pharmacological activities of novel hydrazone derivatives. Indian Journal of Chemistry, **58**:387-402.

Sameemabegum, S.; Prabha, T.; Sribhuvaneswari, S.; Ravisankar, T.; Pavithra, B. and Somasundram, S. (2022). Assessment of the antioxidant and anti-inflammatory activities of *Ipomoea pestigridis* L. leaves. Ann. Phytomed., **11**(2):550-557.

Sarvananda, L. (2018). Short introduction of DNA barcoding. Int. J. Res., **5**(4):673-685.

Shafqat, M.; Qasim, F.; Nasrullah, U.; Ahmad, M.; Hussain, M.; Ali, H. and Qasim, M. W. (2020). DNA barcoding in plants and current molecular issues. Sch. Int. J. Biochem., **3**(03):53-58.

Sivakumar, P.; Monisha, S.; Vijai Selvaraj, K.S.; Chitra, M.; Prabha, T.; Santhakumar, M.; Bharathi, A. and Velayutham, A. (2022). Nutritional value, phytochemistry, pharmacological and *in vitro* regeneration of turmeric (*Curcuma longa* L.): An updated review. Ann. Phytomed., **11**(1):236-246.

Suganthi, S. and Malarvizhi, V. (2020). Phytochemical composition, larvicidal and anti-proliferative effect of *Canavalia virosa*. Int. J. Sci. Res. Sci. Tech., **7**(3):197-206.

Surya, S. and Hari, N. (2017). DNA barcoding of mangroves using ribosomal its marker in rhizophoraceae. Int. J. Sci. Res. Sci. Technol, **3**:606-609.

Teicher, B. A. (2021). TGFβ-directed therapeutics: 2020. Pharmacology and Therapeutics, **217**:107666.

Tian, W.; Chen, C.; Lei, X.; Zhao, J. and Liang, J. (2018). CASTp 3.0: computed atlas of surface topography of proteins. Nucleic Acids Research, **46**(W1), W363-W367.

Xue, V. W.; Chung, J. Y. F.; Cordoba, C. A. G.; Cheung, A. H. K.; Kang, W.; Lam, E. W. F. and Tang, P. M. K. (2020). Transforming growth factor-β: A multifunctional regulator of cancer immunity. Cancers, **12**(11):3099.

Yeddes, W.; Majdi, H.; Gadhoumi, H.; Affes, T. G.; Mohamed, S. N.; Aidi Wannes, W. and Saidani-Tounsi, M. (2022). Optimizing ethanol extraction of rosemary leaves and their biological evaluations. Journal of Exploratory Research in Pharmacology, **7**(2):85-94.

Citation **S. Tamilselvi, N.M. Saravanakumar, G.V. Anjali, V. Gnana Asmi, K. Elango, J. Santhika and T. Prabha (2024). A computational study on anticarcinogenic activity of secondary metabolites in *Salvia rosmarinus* Spenn. against skin cancer. Ann. Phytomed., 13(2):474-483. http://dx.doi.org/10.54085/ap.2024.13.2.47.**